Available online at www.sciencedirect.com
SCIENCE DIRECT®
Journal of Nuclear Materials 329–333 (2004) 524–529
journal of nuclear materials
www.elsevier.com/locate/jnucmat

# Limits on irradiation-induced thermal conductivity and electrical resistivity in silicon carbide materials

L.L. Snead *

*Oak Ridge National Laboratory, Metals and Ceramics Division, ORNL P.O. Box 2008-MS-6087, Oak Ridge, TN 37830-6087, USA*

**Abstract**

Thermal conductivity and electrical resistivity of SiC materials is given for fast neutron fluences up to $7.7\times10^{25}$ n/cm$^2$ at irradiation temperatures of 300, 500 and 800 °C. In situ radiation-induced conductivity is also measured for ionizing dose rates up to ~5 Gy/s (X-ray). Thermal conductivity degradation for CVD SiC is presented in detail exhibiting a substantial reduction from the non-irradiated value of ~370 W/m K. Thermal conductivity of irradiated stoichiometric fiber, CVI SiC matrix composite is also given. A thermal defect resistance approach is used to analyze this data yielding optimum irradiated thermal conductivity for SiC. Neutron irradiation has a permanent, but small effect on electrical conductivity. In the absence of impurity doping effects the neutron damage tends to increase resistivity by less than an order of magnitude. Those SiC materials with electrical resistivities less than ~0.1 S/m undergo little increase in conductivity due to ionizing irradiation, while more than a two order of magnitude increase in electrical conductivity is measured for the highest resistivity form of SiC studied.


## 1. Introduction

Since the early studies of neutron irradiated SiC in support of gas fission reactors, it was recognized that simple defect clusters caused by neutron displacements bring about significant, temperature-dependent swelling and degradation in thermal conductivity [1]. Moreover, neutron damage causes the creation of dangling bonds, which combined with nuclear transmutation of dopants affect electrical conductivity. While swelling and thermal conductivity of SiC composites have been the subject of study for fusion application, their mechanical property changes under irradiation have received the most attention. However, a development program has shown that near-stoichiometric SiC fiber composites exhibit very good mechanical property stability to ~8 dpa for temperatures as high as 800 °C [2]. Noting that swelling and mechanical properties for ceramics tend to saturate by this dose level, present results show promise at higher, fusion relevant doses. This positive development is bringing about a shift in emphasis in the research to address more design-driving questions as discussed by Raffray et al. [3] and Giancarli et al. [4].

This paper gives new information on two critical, design-driving properties. Specifically, data and analysis will be presented related to the limiting maximum thermal conductivity and electrical resistivity to be considered in relation to present day SiC/SiC blanket and first wall design concepts. The importance of thermal conductivity in this regard is widely understood and is not blanket concept-specific. Electrical resistivity has recently been highlighted regarding the potential need for insulating coatings in lithium–lead or other blanket designs using conductive coolants.

## 2. Experimental

Data was generated on various SiC materials for (1) in situ electrical conductivity during exposure to ionizing radiation, (2) post-neutron-irradiation electrical

* Tel.: +1-865 574 9942/423 574 9942; fax: +1-865 241 3650/423 576 8424.
*E-mail address:* sneadll@ornl.gov (L.L. Snead).

0022-3115/$ - see front matter © 2004 Published by Elsevier B.V.
doi:10.1016/j.jnucmat.2004.04.294

Table 1
Properties of materials studied

| Material | Supplier | Processing | Density (g/cc) | Room temp. electrical conductivity $(\Omega\,m)^{-1}$ |
|---|---|---|---|---|
| CVD SiC | Thermoelectron | Chemically vapor deposited (CVD) | 3.1 | 162.0 |
| Alpha SiC | Carborundum (Hexoloy) | Pressureless sintered | 3.1 | $1.32\times10^{-4}$ |
| Beta SiC | Kyocera (SC-221) | Hot pressed | 3.0 | Unknown |
| SiC fiber | Nippon Carbon (Nicalon) | Polymer precursor continuous fiber | 2.6 | $1\times10^{-1}$ |

conductivity, and (3) post-neutron-irradiation thermal conductivity. Physical properties of materials used for the in situ electrical conductivity study are given in Table 1. For the in situ measurements three monolithic materials were machined into discs of 1 mm thickness and approximately 20 mm in diameter. A three electrode 'guard ring' configuration with 50 nm of platinum and >300 nm layer of gold deposited. A single tow of Nicalon fiber was suspended between two ceramic posts. Sample resistance was found by measuring voltage drop across known resistors in series with the specimens with applied voltage (20 V/mm) well below breakdown for these materials. The volume resistivity for the three electrode system following Amey and Hamburger's analysis [5]. The Rensselaer L-band traveling wave electron accelerator was used as the ionizion radiation source whereby packets of 60 MeV electrons impact a tantalum target yielding bremsstrahlung radiation.

Neutron irradiation was carried out in the RB position of the High Flux Isotope Reactor. The highest dose irradiation (~7.7 dpa) was carried out in a thermocouple-controlled capsule. All other samples utilized post-irradiation SiC temperature monitors with an electrical resistivity/isochronal annealing technique [6]. A dose equivalent of 1 dpa $= 1\times10^{25}$ n/m$^2$ ($E > 0.1$ MeV) is assumed for data generated in this work and taken from the literature. Electrical resistivity of neutron irradiated samples was measured using a four-point probe technique. Thermal conductivity was measured using a thermal flash technique assuming a room temperature ($C_p = 667$ J/kg K). Density was found by a density gradient column technique following a bath in hydrofluoric acid to remove surface oxidation.

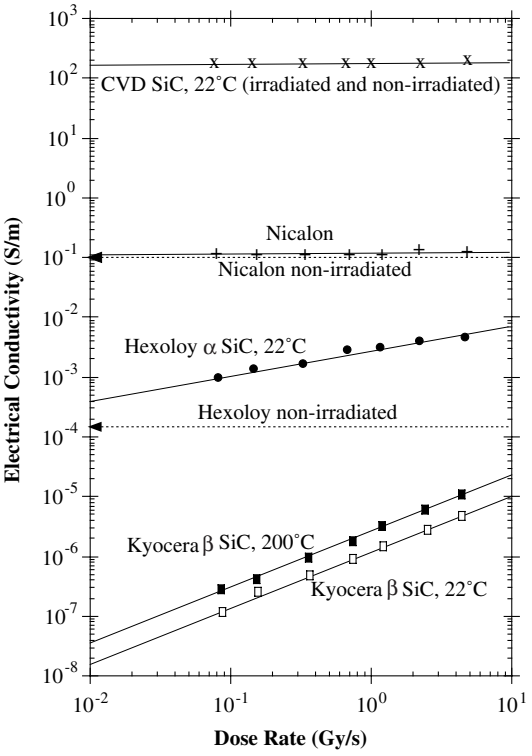


Fig. 1. Radiation enhanced conductivity of select monolithic SiC.

## 3. Results

The effect of ionizing dose rate on the conductivity of monolithic SiC samples is shown in Fig. 1. The CVD SiC (upper curve) was unchanged over the dose range investigated (<5 Gy/s). Nicalon fiber shows a small increase of ~4% for a dose rate of 0.098 Gy/s which increased to 10.5% at 4.73 Gy/s. The lower curves of the figure exhibit the more pronounced radiation enhanced conductivity of sintered α and β SiC. Specifically, the Hexoloy (α) SiC, with non-irradiated conductivity of $1.32\times10^{-4}$ S/m, increases linearly with dose to of $6.14\times10^{-4}$ S/m at 3.05 Gy/s. Kyocera SC-221 β SiC, which possessed the highest initial resistivity, undergoes the greatest increase in conductivity, increasing for both the room temperature and 200 °C irradiations by more than a factor of 30 in both cases between dose rates of 0.086 and 4.2 Gy/s.

The effect of neutron irradiation on post-irradiation room temperature electrical conductivity of composites and Rohm-Haas CVD SiC is given in Table 2.

Table 2
Effect of neutron irradiation on room temperature electrical conductivity of SiC materials

| Fiber/interphase | Conductivity non-irradiated (S/m) | Irradiation condition | Conductivity irradiated (S/m) | Conductivity oxidized (S/m) |
|---|---|---|---|---|
| Type S/Thin PyC | 900 | 7.7 dpa/800 °C | 433 | 479 |
| Type S/Thick PyC | 1700 | 7.7 dpa/800 °C | 915 | 830 |
| Type S/ML SiC | 200 | 7.7 dpa/800 °C | 22 | |
| Type S/Porous SiC | 62 | 7.7 dpa/800 °C | | |
| Rohm-Haas CVD SiC | 20 | 1.1 dpa/300 °C | 10 | – |

Composite materials were unidirectional with conductivity measured in the direction of the fiber length. For the pyrolitic carbon interface samples an 800 °C furnace anneal in air for 8 h was performed to remove the carbon interface. By doing this the contribution of the carbon interphase to the conductivity was eliminated, though it is noted that the conductivity reduction may not be entirely due to carbon as the electrical coupling between fiber and matrix would have been affected in the process. It is also noted that a strong dependence of conductivity on measurement temperature exists for both composite and monolithic SiC. As example, Nicalon Type S fiber/multilayer SiC interphase composite increased in conductivity from 300 S/m at ~20 °C to 590 S/m at 800 °C. Over the same temperature range Type S fiber/(thin) pyrolitic graphite interphase composite increased from 900 to 4800 S/m. Such behavior is typical of semiconductors.

The effect of neutron irradiation on the ambient (~22 °C) thermal conductivity and density of Rohm-Haas CVD SiC is given in Fig. 2 for irradiation temperatures of 300, 500, and 800 °C. From the figure it is not clear that saturation in thermal conductivity or density has occurred for the 800 °C irradiation. While the data are more limited for the lower temperature irradiation it appears that both thermal conductivity and density are near or at saturation at the highest doses. Specifically, ambient thermal conductivity at the highest dose studied for this high-purity fully dense material (3.203 g/cc) has decreased from ~380 (non-irradiated) to 23, 13, and 10 W/m K for 800 °C irradiation, for 800, 500, and 300 °C, respectively. For identically irradiated 2-D plane weave Type S, multilayer SiC interphase materials the thermal conductivity appears to have saturated by a few dpa. Thermal conductivity was measured perpendicular and parallel to the 2-D weave. For the case of Type S/multilayer SiC with ~40% fiber volume fraction and ~15% void the room temperature thermal conductivity thru-thickness was ~12 W/m K and ~20 parallel to the lay-up. At 300 and 500 °C irradiation the room temperature conductivity for this composite was reduced to ~2 W/m K perpendicular, and ~ 5 parallel. For the 800 °C irradiation the thermal conductivities were slightly higher (3 and 6 W/m K, respectively).

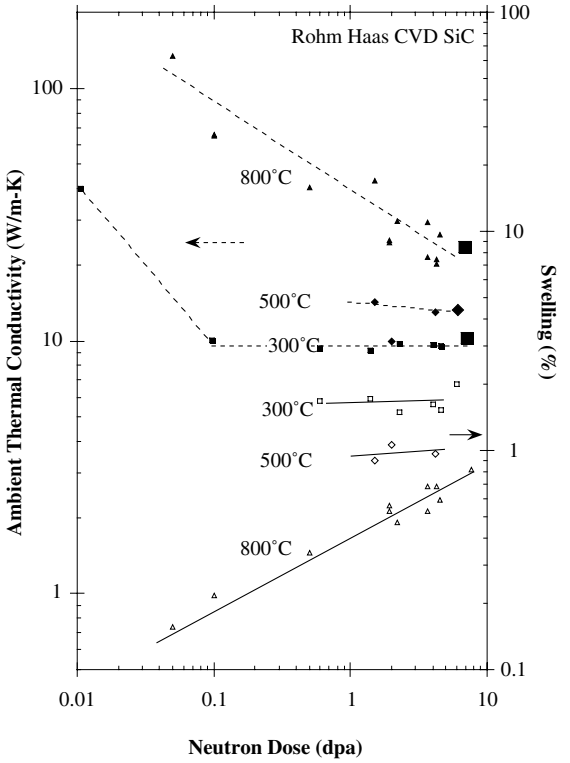


Fig. 2. Room temperature thermal conductivity (filled symbols) and swelling (open symbols) of CVD SiC as a function of neutron dose and irradiation temperature. Large filled symbols are from Youngblood [17].

## 4. Discussion

### 4.1. Electrical resisitivity

Transient increase in electrical conductivity of insulating solids is well understood being studied for a range of materials [7]. This radiation-induced conductivity (RIC), has been studied specifically for alumina and sapphire window applications for the fusion program [8]. In short, any irradiation which imparts sufficient energy to excite the valence electrons may produce RIC,

which is a transient phenomenon. This temporary increase in conductivity is described as $\sigma = \sigma_0 + KR^{\delta}$, where $\sigma_0$ is the base conductivity, $R$ is the ionizing dose rate, and $K$ and $\delta$ are constants depending on irradiation conditions and material. Typically, $\delta$ is somewhere between 0.5 and unity (for oxide ceramics) and is related to electron trapping and has been shown to have a weak temperature dependence [9]. The proportionality constant $K$ is both material and temperature dependent and described [7] as $K$ being proportional to $e_0\mu/\alpha_t N_t E_p$ where $e_0$, $\mu$, and $E_p$ are the electronic charge, summed mobility of electron and holes, and the band gap. The terms $N_t$ and $\alpha_t$ are the trap density and recombination rate. The highly resistive Kyocera β SiC of Fig. 1 exhibits a significant RIC, with $K = 1.25 \times 10^{-6}$ (S s/Gy m) and $\delta$ of 0.9. While the value of $\delta$ is consistent with the oxide ceramics, the $K$ value is substantially higher than the $10^{-12}$–$10^{-9}$ (S s/Gy m) levels seen in the oxide insulators. Furthermore, the more conductive Hexoloy materials ($\delta$ of 0.5) has an even greater difference with $K = 2.27 \times 10^{-3}$ (S s/Gy m). It is noted that the Kyocera material has substantial non-SiC 'glassy phases' formed by sintering binders which typically increase resistivity. However, as the materials increase in conductivity essentially no RIC was noted indicating that the Fermi level for the higher conductivity materials induced greater thermally stimulated electrons as compared to the ionized electron contribution.

Several competing factors contribute to the change in the as-irradiated (permanent) conductivity change in SiC. For example, nuclear transmutation doping will occur, increasing donor concentration through the $^{30}Si(n,\gamma)^{31}Si$ and subsequent β-decay to (n-type donor) $^{31}P$. Additionally, 20% of the 290 wppm intrinsic (p-type) boron present in the commercial Rohm-Haas CVD SiC is removed during reactor irradiation due to the $^{10}B(n,\alpha)^{7}Li$ reaction. The result of change in doping level in the CVD SiC is to effectively increase resistivity. At the same time, elastic collisions between high-energy neutrons and the lattice produce simple point defects, increasing the dangling bond density, decreasing conductivity. Upon annealing dangling bonds are removed and the material resitivity increases substantially [10]. Results shown in Table 2 clearly indicate an increase in resistivity for both CVD SiC and composite materials following neutron irradiation.

Due to the level of immaturity in fusion reactor SiC/SiC blanket designs an absolute upper limit on electrical conductivity for SiC composite does not exist. A value of 500 S/m has been suggested to be acceptable [11] based on analysis of the European TAURO design. Furthermore, Scholz et al. [12] calculated the magnetohydrodynamic pressure increase (hence pumping power increase) for the lithium cooled, SiC/SiC TAURO blanket to be about a factor of two for a conductivity of 500 S/m at 750 °C. This value of conductivity was assumed based on the commercial Cerasep SiC composite, which increases in conductivity by ~60% from room temperature to 750 °C [12]. Composites in the present study showed similar magnitude increase in conductivity with temperature and the permanent effect of irradiation is seen to decrease conductivity therefore can be ignored. The in situ radiation-induced conductivity (Fig. 1) also appears not to be an issue. This conclusion can be drawn by extrapolated Fig. 1 data to fusion relevant dose levels (~$10^4$ Gy/s). It is noted that RIC for oxide ceramics has been shown to be linear over such a dose range, therefore extrapolation is considered appropriate. In this case the electrical conductivity is still well under the 500 S/m value.

### 4.2. Thermal conductivity

Due to a low density of valence band electrons, thermal conductivity of ceramic materials is based on phonon transport. For each ceramic the ease of conducting heat can be described by the strength of the individual contributors to phonon scattering: grain boundary scattering $(1/K_{gb})$, phonon–phonon interaction (or umklapp scattering $1/K_u$), and defect scattering $(1/K_d.)$ Because scattering for each of these elements occurs at differing phonon frequencies and can be considered *separable*, the summed thermal resistance for a material can be simply described as the summation of the individual elements; i.e., $1/K = 1/K_{gb} + 1/K_u + 1/K_d$. The effect of irradiation on ceramics at low homologous temperature is to produce simple defects and defect clusters that very effectively scatter phonons. For ceramics processed for high thermal conductivity the irradiation-induced defect scattering quickly dominates with saturation thermal conductivity typically achieved by a few dpa. Moreover, as the irradiation-induced defect scattering exceeds the phonon–phonon scattering, the temperature dependence of thermal conductivity is much reduced or effectively eliminated. It is noted that the 300 and 500 °C irradiation of this study yielded constant thermal conductivity values as measured from room temperature to the irradiation temperature. However, the 800 °C irradiated material has slightly lower thermal conductivity as measured at 800 °C compared room temperature value indicating that phonon scattering was still competing. It is also noted (cf. Fig. 2) that the 800 °C irradiation does not indicate saturation conductivity and that a (small) temperature dependence of thermal conductivity remains. Even so, the room temperature thermal conductivity for all three irradiation temperatures is quite close to the conductivity measured at the irradiation temperature. Referring to the 800 °C values of swelling in Fig. 2 it is noted that saturation must be close in that the swelling values are approaching the 500 °C swelling values and the 600 °C saturation swelling data generated using single ion irradiation [13].

Given the assumption of separability, and further assuming that irradiation-induced defects dominate intrinsic defects ($1/K_d$), an irradiation-induced defect resistance term can be defined: $1/K_{rd} = 1/K_{irr} - (1/K_u + 1/K_{gb}) = 1/K_{irr} - 1/K_{non\text{-}irr}$. This thermal defect resistance term is the material response to irradiation in the absence grain boundary alteration or other factors such as internal cracking. It has been shown [14] that for doses where the defect scattering dominates the umklapp scattering, the defect resistance is proportional to the square root of the vacancy defect concentration. As this term is independent of starting thermal conductivity, if it is assumed that the surviving vacancy clusters in a material type (e.g. CVD SiC) are independent of intrinsic defects or impurities, the thermal defect resistance term as a function of temperature can be applied to any CVD SiC to estimate the final irradiated thermal conductivity.

Fig. 3 gives a compilation of thermal defect resistance for highly irradiated, near fully dense high-purity CVD SiC. Using data from this study, Price [15], Senor [16], and Youngblood [17]. The published data for siliconized and hot pressed materials were omitted due to the presence of sintering aids that potentially alter grain boundary scattering upon irradiation. Error bars were calculated based on information provided by the authors, or assumed. Room temperature thermal conductivities (given in legend) of 288 W/m K were assumed [18] for the work of Youngblood [17] and Senor [16].

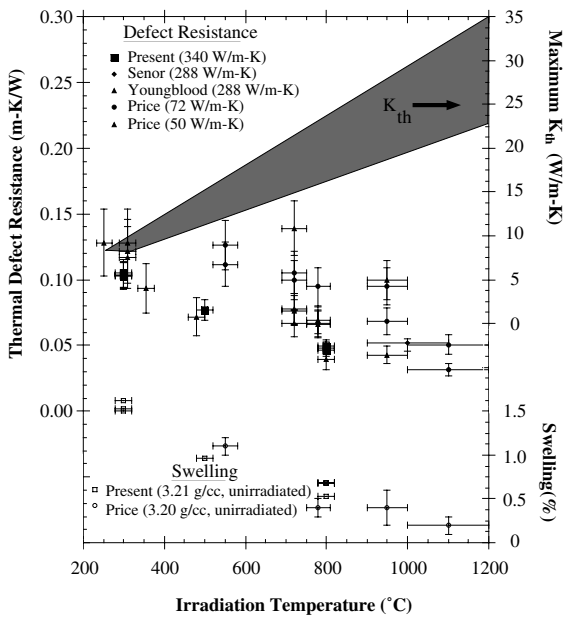


Fig. 3. Thermal defect resistance (filled symbols) and swelling (open symbols) of irradiated CVD SiC. The plot includes data from Refs. [15–17].

However, error in this assumption would not have had significant effect on calculated thermal resistance due to the high starting thermal conductivities.

It is interesting to note that if the thermal defect resistance data of this study is normalized to swelling (i.e. $(1/K_{rd})$/%swell) and plotted as a function of irradiation temperature, a constant value is obtained. This implies that over the temperature range of this study (300–800 °C) the defects that govern thermal conductivity and swelling are the same and do not change over this temperature range. This will likely not be the case for irradiation temperatures >800 °C as the microstructure becomes dominated by interstitial loops.

From Fig. 3 the density decrease (driven by interstitial defect strain) upon irradiation for this work and that of Price [15] were measured in similar fashion and are in good agreement. However, while the thermal defect resistance data is consistent for this work and the work of Youngblood [17] and Senor [16], the Price [15] data is somewhat higher. Assuming no experimental error, this suggests there may be a difference in the vacancy complex formation for the lower density, lower conductivity material of Price [15]. Though not discussed by the authors, it is possible that the lower density of Price's material may have been due to excess atomic silicon. Also plotted in Fig. 3 is the ideal, or maximum saturated thermal conductivity band, as a function of irradiation temperature. This band has simply inverted the thermal defect resistance data from this study as well as the data of Youngblood [17] and Senor [16] (all Morton/Rohm-Haas CVD SiC). This is therefore the thermal conductivity dominated solely by the irradiation-induced vacancy clusters, and the room temperature thermal conductivity can be assumed to be near the thermal conductivity measured at the irradiation temperature. It is seen that irradiated saturation thermal conductivity increases from a value of ~7 W/m K at 200 °C to 20–27 W/m K for 1000 °C irradiation. The wide range at the elevated temperature may be due to a non-saturated value of thermal conductivity for the present work and that of Youngblood [17] which was in the dose range of 4–8 dpa as compared to that of Senor [16] taken as ~26 dpa. A saturation value closer to 20 W/m K is therefore likely.

Required thermal conductivity for fusion reactor design is somewhat different for the recent design studies and dependent on the design and the area of application (i.e. divertor, first wall, blanket, or magnet structure). However, the TAURO, DREAM, and ARIES designs [3] have assumed through thickness values of thermal conductivity of 15, 15–60, and 20 W/m K at ~1000 °C, respectively. The present plane weave Type S fiber, CVI SiC composite irradiated in HFIR in the range of 2–4 dpa yields thru-thickness room temperature conductivity in the range of 2–3 W/m K in the irradiation temperature range of 300–800 °C where similarly infiltrated Sylramic fiber composite resulted in room temperature

conductivity of ~5 W/m K [17]. There are several composites which match or exceed the non-irradiated conductivity of the material of this study, and further improvement will occur by adopting processing using higher crystallinity fibers, higher processing temperatures leading to lower vacancy concentration, lower matrix void fraction, and optimization of the fiber/matrix interphase for reduced boundary scattering. However, the optimum thermal conductivity cannot exceed that given in Fig. 3, and given the intrinsic need for the fiber/matrix interface and the microcracking of composite materials, the conductivity will necessarily be lower than depicted in Fig. 3. For these reasons the thermal conductivities assumed in the present SiC/SiC core design appear overly optimistic.

## 5. Conclusions

(1) Electrical conductivity of SiC composites is a function of initial processing choices of fiber, matrix and interphase. Fabrication of composites with substantially lower conductivity than the 500 S/m TAURO assumed upper allowed limit should not pose a problem. Materials in this study manufactured with the radiation-stable Type S Nicalon and ICVI SiC matrix infiltration gave room temperature electrical conductivity ranging from 60 to 1700 S/m, depending on interphase chosen, though the matrix conductivity may have been different. The effect of temperature on conductivity, as has been shown previously for Cerasep SiC, increases by less than a factor of two. At this level of conductivity the material is about four orders of magnitude higher than where radiation-induced conductivity would become of concern for fusion blankets. Neutron displacement damage will also alter electrical resistivity, though this will decrease the resistivity of the material and therefore improve MHD performance. This permanent reduction was seen to be about a factor of two for the materials in this study.

(2) The thermal conductivity for very high-purity CVD SiC has been used as a model to calculate the material-dependent thermal defect resistance for SiC. Using irradiated data in this paper at 300, 500 and 800 °C, along with data on similar material from the literature, a formalism for describing thermal conductivity reduction based on the assumption of separability of phonon-scattering centers has been adopted. Using this formalism the maximum saturation thermal conductivity for SiC is given to be ~7 W/m K for 200 °C increasing to ~20–27 W/m K for 1000 °C irradiation. Due to the intrinsic internal interfaces of composite materials the as-irradiated thermal conductivity will be less than these values. The conclusion of this analysis is that present day assumptions for the thermal conductivity of SiC/SiC composites in fusion reactor designs are overly optimistic.

## References

[1] R.J. Price, J. Nucl. Mater. 33 (1969) 17.
[2] T. Hinoki et al., J. Nucl. Mater. 307–311 (2003) 1157.
[3] A.R. Raffray et al., Fus. Eng. Des. 55 (2001) 55.
[4] L. Giancarli, H. Golfier, Y. Poitevin, J.F. Salavy, Report SERMA/LCA/RT/99-2677/A, 1999.
[5] W.G. Amey, J.F. Hamburger, Proc. Am. Soc. Test. Mater. 49 (1949) 1079.
[6] L.L. Snead, A.M. Williams, A.L. Qualls, in: M.L. Grossbeck et al. (Eds.), The Effects of Radiation on Materials: 21st International Symposium, ASTM STP 1447, ASTM International, West Conshohocken, PA, in press.
[7] V.A.J. van Lint et al., in: Mechanisms of Radiation Effects in Electronic Materials, vol. 1, John Wiley, New York, 1980.
[8] L.W. Hobbs, F.W. Clinard Jr., S.J. Zinkle, R.C. Ewing, J. Nucl. Mater. 216 (1994) 291.
[9] G.P. Pells, J. Nucl. Mater. 155–157 (1988) 67.
[10] L.L. Snead, S.J. Zinkle, Nucl. Instrum. and Meth. B 191 (2002) 497.
[11] L. Giancarli et al., Fus. Eng. Des. 48 (2000) 509.
[12] R. Scholz, J.d. Greef, C. Vinche, in: B. Beaumont et al. (Eds.), 20th Symposium on Fusion Technology, Marseille, France, 2, 1998, p. 11675.
[13] H. Kishimoto, PhD thesis, Institute for Advanced Energy, Kyoto, 2002.
[14] D.P. White, personal communication, 2004.
[15] R.J. Price, J. Nucl. Mater. 46 (1973) 268.
[16] D.J. Senor et al., Fus. Technol. 30 (1996) 943.
[17] G.E. Youngblood, D.J. Senor, R.H. Jones, Fusion Materials Semiannual Progress Report DOE/ER-0313/33, 2002.
[18] G.E. Youngblood, personal communication, 2004.